

Quantum spin ladders at $T=0$ and at high temperatures studied by series expansions

J. Oitmaa*

School of Physics, The University of New South Wales, Sydney, New South Wales 2052, Australia

Rajiv R. P. Singh[†]

Department of Physics, University of California, Davis, California 95616

Zheng Weihong[‡]

School of Physics, The University of New South Wales, Sydney, New South Wales 2052, Australia

(Received 7 February 1996)

We have carried out extensive series studies, at $T=0$ and at high temperatures, of two-chain and three-chain spin-half ladder systems with antiferromagnetic intrachain and both antiferromagnetic and ferromagnetic interchain couplings. Our results confirm the existence of a gap in the two-chain Heisenberg ladders for all nonzero values of the interchain couplings. Complete dispersion relations for the spin-wave excitations are computed. For three-chain systems, our results are consistent with a gapless spectrum. We also calculate the uniform magnetic susceptibility and specific heat as a function of temperature. We find that as $T \rightarrow 0$, for the two-chain system the uniform susceptibility goes rapidly to zero, whereas for the three-chain system it approaches a finite value. These results are compared in detail with previous studies of finite systems. [S0163-1829(96)06226-1]

I. INTRODUCTION

The magnetic properties of low dimensional systems have been the subject of intense theoretical and experimental research in recent years. It is by now well established that one-dimensional Heisenberg antiferromagnets with integer spin have a gap in the excitation spectrum, whereas those with half-integer spin have gapless excitations. The former have a finite correlation length, while for the latter it is infinite with the spin-spin correlation function decaying to zero as a power law. In two dimensions, the unfrustrated square-lattice Heisenberg model has long range Néel order in the ground state. It has gapless Goldstone modes as expected. In recent years much interest has focused on systems with intermediate dimensionality and on questions of crossovers between $d=1$ and $d=2$. One approach to this problem has been to study a two-dimensional system where the coupling for the spins separated along the x axis is different from that for those separated along the y axis.¹ It has been suggested that an alternative way to explore this issue is through the Heisenberg spin ladders consisting of a finite number of chains coupled together, with a coupling J_{\parallel} along the chains and J_{\perp} between them. These systems have been the subject of considerable recent theoretical and experimental interest.

Experimentally, two-chain $S=\frac{1}{2}$ ladders are realized in vanadyl pyrophosphate $(\text{VO})_2\text{P}_2\text{O}_7$ (Ref. 2) and in the strontium cuprate SrCu_2O_3 ,³ whereas three-chain $S=\frac{1}{2}$ ladders are realized in the strontium cuprate SrCu_3O_5 .³

Theoretically, a number of striking predictions have been made for such systems. These have been recently reviewed by Dagotto and Rice.⁴ Barnes *et al.*^{5,6} carried out extensive Monte Carlo studies of the excitation spectrum and the magnetic susceptibility for two-chain ladders with antiferromagnetic interchain coupling. White *et al.*⁷ and Hida⁸ have used

the density-matrix renormalization method to study the spin gap. Watanabe⁹ has applied the numerical diagonalization method to finite systems of two-chain ladders with ferromagnetic interchain coupling. Azzouz *et al.*¹⁰ developed a mean-field theory and used the density-matrix renormalization group method to study two-chain ladders. Gopalan, Rice, and Sigrist¹¹ presented a variational wave function for the ground state of the two-leg ladder. The extension of the Lieb-Shultz-Mattis theorem to odd-chain ladders by Affleck¹² and Rojo¹³ implies that spin ladders with odd numbers of legs have either degenerate ground states or gapless excitations. Troyer *et al.*¹⁴ have used improved versions of the quantum transfer-matrix algorithm to study the temperature dependence of the susceptibility, specific heat, correlation length, etc. of two-chain ladders. Finite-size scaling was used by Hatano and Nishiyama¹⁵ for multileg ladders, and recently Frischmuth *et al.*¹⁶ and Sandvik *et al.*¹⁷ have applied quantum Monte Carlo simulation to compute the temperature dependence of the uniform susceptibility and internal energy for spin ladders with up to six legs. One clear result from all these studies is that ladders with an even number of legs have an energy gap, short range correlation and a ‘‘spin liquid’’ ground state. On the other hand, ladders with an odd number of legs have gapless excitations, quasi long range order, and a power-law falloff of spin-spin correlations, similar to single chains. Experiments also confirm these features.

We have carried out extensive series studies of two-chain and three-chain ladder systems with both antiferromagnetic and ferromagnetic interchain coupling J_{\perp} , via Ising expansions and dimer expansions at $T=0$, and also by high temperature series expansions. Our results confirm the existence of a gap in the two-chain system and delineate the phase diagram in the parameter space of Ising anisotropy and the parameter ratio J_{\perp}/J_{\parallel} . The complete spin-wave excitation spectra are computed. For the three-chain system we are

unable to exclude the possibility of a gap from a direct calculation of the excitation spectra. However, several other calculations, such as the phase boundary with Ising anisotropy and uniform susceptibility, led us to the conclusion that the spectrum for the three-chain system is gapless. In addition, we develop a high temperature series expansion for the uniform magnetic susceptibility and the specific heat for two-chain and three-chain systems with $J_{\parallel}=J_{\perp}$; the susceptibility of two-chain ladders is as expected for a system with a spin gap while that of three-chain ladders appears to remain finite in the zero-temperature limit, suggesting the absence of a spin gap. We compare our results in detail with previous calculations.

II. SERIES EXPANSIONS

The Hamiltonian of a spin ladder with n_l legs is given by

$$H = J_{\parallel} \sum_{i,l=1}^{l=n_l} \mathbf{S}_{l,i} \cdot \mathbf{S}_{l,i+1} + J_{\perp} \sum_{i,l=1}^{l=n_l-1} \mathbf{S}_{l,i} \cdot \mathbf{S}_{l+1,i} \quad (1)$$

where $\mathbf{S}_{l,i}$ denotes the $S=1/2$ spin at the i th site of the l th chain. J_{\parallel} is the interaction between nearest neighbor spins along the chain and J_{\perp} is the interactions between nearest neighbor spins along the rungs. We denote the ratio of couplings as y , that is, $y \equiv J_{\perp}/J_{\parallel}$. In the present paper the intra-chain coupling is taken to be antiferromagnetic (that is, $J_{\parallel} > 0$) whereas the interchain coupling J_{\perp} can be either antiferromagnetic or ferromagnetic. This includes the values of interest in the experimental systems discussed earlier where $J_{\perp} \sim J_{\parallel}$. Without loss of generality, we can set $J_{\parallel} = 1$ hereafter.

We have carried out three different expansions for the system. The first is the expansion about the Ising limit at zero temperature for both two- and three-chain ladders. We have computed the ground state properties as well as the spin-wave excitation spectra by this expansion. The second is the dimer expansion, again at $T=0$. This expansion can be done for the two-chain system with antiferromagnetic interchain coupling only. The third is the high temperature series expansion for the uniform susceptibility of the two-chain and three-chain ladders with $y=1$.

A. Ising expansions

To perform an expansion about the Ising limit for this system, we introduce an anisotropy parameter x , and write the Hamiltonian in Eq. (1) as

$$H = H_0 + xV \quad (2)$$

where

$$\begin{aligned} H_0 &= \sum_{i,l=1}^{l=n_l} S_{l,i}^z S_{l,i+1}^z + y \sum_{i,l=1}^{l=n_l-1} S_{l,i}^z S_{l+1,i}^z, \\ V &= \sum_{i,l=1}^{l=n_l} (S_{l,i}^x S_{l,i+1}^x + S_{l,i}^y S_{l,i+1}^y) \\ &\quad + y \sum_{i,l=1}^{l=n_l-1} (S_{l,i}^x S_{l+1,i}^x + S_{l,i}^y S_{l+1,i}^y). \end{aligned} \quad (3)$$

The limits $x=0$ and $x=1$ correspond to the Ising model, and the Heisenberg model respectively. The operator H_0 is taken as the unperturbed Hamiltonian, with the unperturbed ground state being the usual Néel state for antiferromagnetic interchain coupling, and a fully ordered collinear state for ferromagnetic interchain coupling. The operator V is treated as a perturbation. It flips a pair of spins on neighboring sites. The Ising expansion method has been previously reviewed in several articles,^{18,19} and will not be repeated here. The calculations involved a list of 9184 linked clusters of up to 16 sites for the two-chain ladder, and 14 082 linked clusters of up to 12 sites for the three-chain ladder, together with their lattice constants and embedding constants.

Series have been calculated for the ground state energy per site E_0/N , the staggered magnetization M for $y > 0$ (or collinear magnetization M for $y < 0$), the parallel staggered/collinear susceptibility χ_{\parallel} , and the uniform perpendicular susceptibility χ per site for several ratio of couplings $y = \pm 0.1, \pm 0.25, \pm 0.5, \pm 0.75, \pm 1, \pm 1.5, \pm 2, \pm 4, \pm 8$ up to order x^{16} for two-chain ladders, and x^{12} for three-chain ladders (the series for uniform perpendicular susceptibility χ is one order less in each case). The resulting series for $y = \pm 1$ for the two-chain and three-chain systems are listed in Tables I and II; the series for other value of y are available on request.

To analyze these series, we first performed a standard Dlog Padé analysis of the magnetization M and parallel susceptibility χ_{\parallel} series. We found that for two-chain ladders, the series lead to a simple power-law singularity at $x < 1$:

$$M \sim (1 - x/x_c)^{\beta}, \quad \chi_{\parallel} \sim (1 - x/x_c)^{-\gamma}, \quad (4)$$

with the indices β and γ close to $1/8$ and $7/4$, respectively. This transition at $x < 1$, with criticality in the universality class of the two-dimensional (2D) Ising model, is strong evidence that in the Heisenberg limit the system has a disordered ground state with a spin gap, as is the case for the spin-1 chain.²⁰ In contrast, for the three-chain ladders, the series analysis showed poor convergence and suggested a singularity at $x \geq 1$. This implies that for the three-chain ladders, the system is analogous to the spin-half chain, with gapless spectra and power-law correlations in the Heisenberg limit.

Figure 1 shows the phase boundary for two-chain ladders as a function of y . It is interesting to note the different behavior for $y > 0$ and for $y < 0$: for antiferromagnetically coupled two-chain ladders ($y > 0$), x_c decreases as y increases, and in the limit of $y \rightarrow \infty$, x_c will approach 0. But for ferromagnetically coupled two-chain ladders ($y < 0$), x_c first decreases as the absolute value of y increases from zero, but then the trend reverses and it, once again, approaches 1 as $y \rightarrow -\infty$. To understand this behavior, we can map the system for large negative y to a spin-1 chain with on-site (single-ion) anisotropy:

$$H = \frac{1}{2} \sum_i [\mathbf{S}_{i,\text{tot}} \cdot \mathbf{S}_{i+1,\text{tot}} + y(1-x)(S_{i,\text{tot}}^z)^2] \quad (5)$$

where $\mathbf{S}_{i,\text{tot}}$ denotes the $S=1$ spin at the i th site of the chain. We can get the asymptotic behavior of the phase boundary in the limit of $y \rightarrow -\infty$ by studying the following spin-1 chain with on-site anisotropy:

TABLE I. Series coefficients for the ground state energy per site E_0/N , the staggered/collinear magnetization M , and staggered parallel susceptibility χ_{\parallel} . Coefficients of x^n are listed for both the spin-1/2 two-chain and three-chain ladders with $y = \pm 1$.

n	E_0/N	M	χ_{\parallel}
Two-chain ladders with $y = -1$			
0	-3/8	1/2	0
2	$-1.250000000000 \times 10^{-1}$	$-1.250000000000 \times 10^{-1}$	$2.500000000000 \times 10^{-1}$
4	$-1.562500000000 \times 10^{-2}$	$-6.944444444444 \times 10^{-2}$	$4.131944444444 \times 10^{-1}$
6	$2.443214699074 \times 10^{-3}$	$1.398473668981 \times 10^{-3}$	$9.964453526878 \times 10^{-2}$
8	$-3.391054004308 \times 10^{-3}$	$-4.293584111636 \times 10^{-2}$	$6.561704135203 \times 10^{-1}$
10	$-3.083929459431 \times 10^{-4}$	$-9.459983497527 \times 10^{-3}$	$2.592402875212 \times 10^{-1}$
12	$-5.758725813964 \times 10^{-4}$	$-2.517788286146 \times 10^{-2}$	$8.633367551243 \times 10^{-1}$
14	$-3.508609329659 \times 10^{-4}$	$-1.290819523741 \times 10^{-2}$	$5.194241039530 \times 10^{-1}$
16	$-3.658331257827 \times 10^{-4}$	$-2.220489673071 \times 10^{-2}$	1.197591274920
Two-chain ladders with $y = 1$			
0	-3/8	1/2	0
2	$-1.875000000000 \times 10^{-1}$	$-1.875000000000 \times 10^{-1}$	$3.750000000000 \times 10^{-1}$
4	$-9.114583333333 \times 10^{-3}$	$-1.176215277778 \times 10^{-1}$	$9.751157407407 \times 10^{-1}$
6	$-6.564670138889 \times 10^{-3}$	$-1.298255449460 \times 10^{-1}$	2.225074548290
8	$-1.011191788034 \times 10^{-2}$	$-2.567768064481 \times 10^{-1}$	6.466470614293
10	$-4.438918908655 \times 10^{-3}$	$-3.308567310261 \times 10^{-1}$	$1.436049594755 \times 10^1$
12	$-1.149045736404 \times 10^{-2}$	$-6.754838729347 \times 10^{-1}$	$3.661634831290 \times 10^1$
14	$-9.014538657677 \times 10^{-3}$	-1.059678748481	$8.236161272382 \times 10^1$
16	$-1.860424772341 \times 10^{-2}$	-2.087462804052	$1.962459013257 \times 10^2$
Three-chain ladders with $y = -1$			
0	-5/12	1/2	0
2	$-1.111111111111 \times 10^{-1}$	$-1.018518518519 \times 10^{-1}$	$1.913580246914 \times 10^{-1}$
4	$-9.126984126984 \times 10^{-3}$	$-2.765516082976 \times 10^{-2}$	$1.235451495119 \times 10^{-1}$
6	$-3.430007743753 \times 10^{-3}$	$-2.229002861112 \times 10^{-2}$	$1.702591936321 \times 10^{-1}$
8	$-4.479840217373 \times 10^{-4}$	$-6.778016397592 \times 10^{-3}$	$9.228960192872 \times 10^{-2}$
10	$-1.150888174205 \times 10^{-3}$	$-1.348552579039 \times 10^{-2}$	$1.814452046940 \times 10^{-1}$
12	$-5.493987828590 \times 10^{-4}$	$-9.549725222639 \times 10^{-3}$	$1.785680892107 \times 10^{-1}$
Three-chain ladders with $y = 1$			
0	-5/12	1/2	0
2	$-1.777777777778 \times 10^{-1}$	$-1.551851851852 \times 10^{-1}$	$2.766913580247 \times 10^{-1}$
4	$2.099353321576 \times 10^{-3}$	$-3.010635013951 \times 10^{-2}$	$2.520792079948 \times 10^{-1}$
6	$-5.486291040711 \times 10^{-3}$	$-4.567138485811 \times 10^{-2}$	$4.781602664625 \times 10^{-1}$
8	$-9.770232257758 \times 10^{-4}$	$-2.676534614009 \times 10^{-2}$	$5.289125611753 \times 10^{-1}$
10	$-8.540222317364 \times 10^{-4}$	$-2.413110830174 \times 10^{-2}$	$6.371032432384 \times 10^{-1}$
12	$-7.963887426932 \times 10^{-4}$	$-3.026105625065 \times 10^{-2}$	1.024475965994

$$H = \frac{1}{2} \sum_i [S_{i,\text{tot}}^z S_{i+1,\text{tot}}^z - c(S_{i,\text{tot}}^z)^2 + x'(S_{i,\text{tot}}^x S_{i+1,\text{tot}}^x + S_{i,\text{tot}}^y S_{i+1,\text{tot}}^y)]. \quad (6)$$

For this model, we have carried out series expansions in x' to order x'^{14} (i.e., 14 sites) for staggered magnetization M for several different values of c : $c = 0.275, 0.29, 0.3, 0.325$, and performed a standard Dlog Padé analysis to find the critical value c' which gives the singularity of M at $x' = 1$. We get $c' = 0.29(1)$. Hence, the asymptotic behavior of the phase boundary in the limit $y \rightarrow -\infty$ is given by

$$x_c = 1 + 0.29/y \quad (7)$$

which is also shown in Fig. 1 as a bold line near $y/(1+|y|) = -1$.

Figure 2 gives the results of the ground state energy per site E_0/N versus y for both two-chain and three-chain ladders at the Heisenberg point $x = 1$. Our results for the ground state energy agree extremely well with the recent quantum Monte Carlo simulation.¹⁶ In Fig. 3, we present the uniform perpendicular susceptibility at $T=0$.

We also performed the Ising expansion for the triplet spin-wave excitation spectrum of two-chain and three-chain ladders using Gelfand's method.²¹ To overcome a possible singularity at $x < 1$ in the two-chain ladders, and to get a better convergent series in the Heisenberg limit, we add the following staggered field term to the Hamiltonian in Eq. (2):

TABLE II. Series coefficients for the perpendicular susceptibility χ_{\perp} . Coefficients of x^n are listed for two-chain and three-chain ladders with $y = \pm 1$.

n	Two-chain $y = -1$	Two-chain $y = 1$	Three-chain $y = -1$	Three-chain $y = 1$
0	1/3	1/3	11/36	11/36
1	-2/9	-1/2	-1/6	-13/30
2	$1.481481481481 \times 10^{-2}$	$5.666666666667 \times 10^{-1}$	$1.266534391534 \times 10^{-2}$	$4.652226631393 \times 10^{-1}$
3	$5.308641975309 \times 10^{-3}$	$-7.143518518519 \times 10^{-1}$	$-1.112134668682 \times 10^{-2}$	$-5.160474965706 \times 10^{-1}$
4	$-2.120002939447 \times 10^{-2}$	$7.544920634921 \times 10^{-1}$	$1.134331580417 \times 10^{-2}$	$5.434191826896 \times 10^{-1}$
5	$7.283052502380 \times 10^{-2}$	$-9.203876999874 \times 10^{-1}$	$-2.787971676358 \times 10^{-2}$	$-6.037870527565 \times 10^{-1}$
6	$-6.507519406167 \times 10^{-2}$	$9.542443240384 \times 10^{-1}$	$3.588831815932 \times 10^{-2}$	$6.192643274088 \times 10^{-1}$
7	$-9.850515124711 \times 10^{-3}$	-1.220670122297	$-3.496516710785 \times 10^{-2}$	$-6.538548959720 \times 10^{-1}$
8	$-3.321642365298 \times 10^{-3}$	1.243330662897	$3.361956127668 \times 10^{-2}$	$6.836898452099 \times 10^{-1}$
9	$3.225303151489 \times 10^{-2}$	-1.570424359869	$-4.583945317287 \times 10^{-2}$	$-7.207963780768 \times 10^{-1}$
10	$-2.164319811625 \times 10^{-2}$	1.612928972471	$4.084885561076 \times 10^{-2}$	$7.446415246323 \times 10^{-1}$
11	$-2.229164879943 \times 10^{-2}$	-2.181953857121	$-4.495109043570 \times 10^{-2}$	$-7.944909220697 \times 10^{-1}$
12	$-8.386607266663 \times 10^{-3}$	2.245984866808		
13	$1.980513341011 \times 10^{-2}$	-3.034629087270		
14	$-1.128439840082 \times 10^{-2}$	3.158070079722		
15	$-1.625818723347 \times 10^{-2}$	-4.546560413718		

$$\Delta H = t(1-x) \sum_i (-1)^i S_i^z. \quad (8)$$

ΔH vanishes at $x=1$. We adjust the coefficient t to get the smoothest terms in the series, with a typical value being $t=2$. We computed the Ising expansion for the triplet spin-wave excitation spectrum $\epsilon(k)$ up to order x^{15} for two-chain ladders, and up to order x^{11} for three-chain ladders. These series are too long to be listed here, but are available on request.

These series have been analyzed by using integrated first-order inhomogeneous differential approximants.²² For the two-chain ladder, there are two bands of excitations; Fig. 4 shows the dispersion $\epsilon(k)$, with $k_y = \pi$, for antiferromagnetic interchain coupling. The other band with $k_y = 0$ is related to this by $\epsilon(k_x, 0) = \epsilon(\pi - k_x, \pi)$. This is simply due to the staggered field, which doubles the spectrum. As a com-

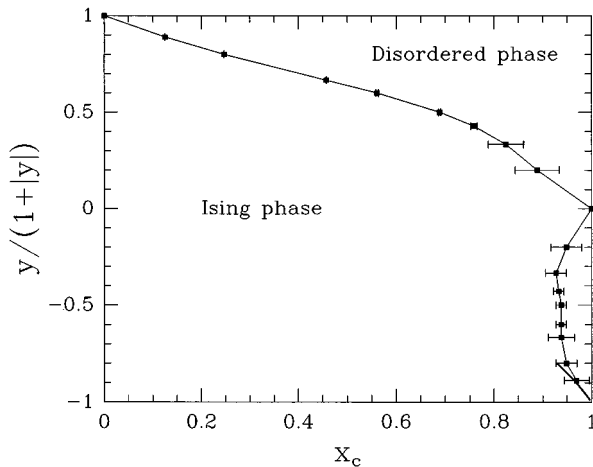


FIG. 1. The phase boundary for two-chain ladder. The asymptotic behavior as $y \rightarrow -\infty$ predicted by a spin-1 single chain system with on-site anisotropy is also shown by the bold line.

parison, the dispersion relation of a single chain (that is, the case of $y=0$) is also shown. It can be seen from the graph that in the limit $y \rightarrow 0$, the dispersion relation has a simple cosine function with a period of 2π , and in the limit $y \rightarrow \infty$, the dispersion relation also has a simple cosine form with a period of 4π , and a gap in the spectrum. Barnes and Riera⁶ argued that the dispersion, for all y , can be fitted by combining these two functions into the following form:

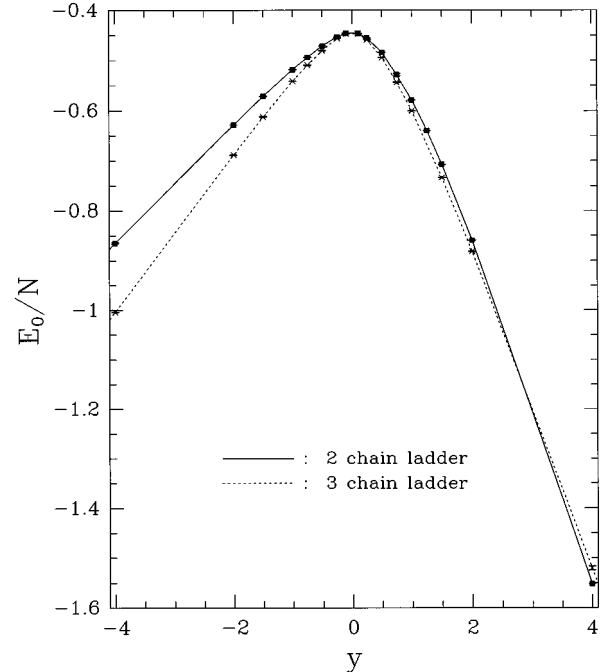


FIG. 2. The ground state energy per site E_0/N as function of y for two-chain and three-chain ladders. The results for a two-chain ladder with $y \geq 1$ are from the dimer expansions, and the rest of the results are from the Ising expansions. The error bars are much smaller than the symbols.

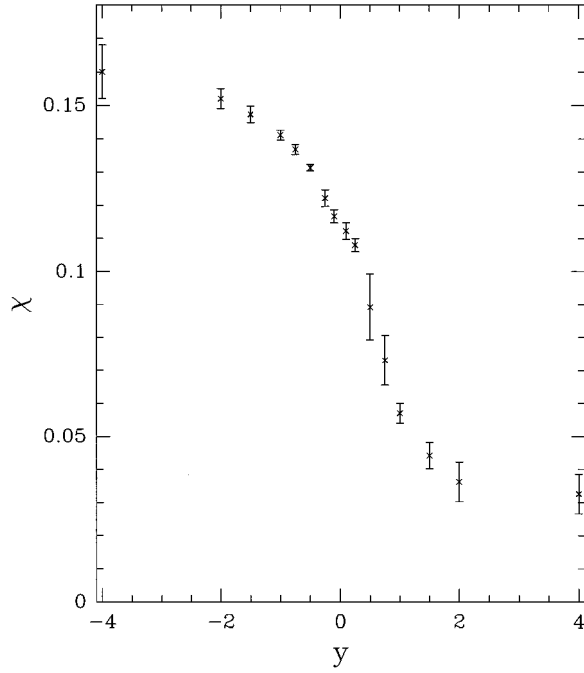


FIG. 3. The uniform susceptibility χ at $T=0$ as a function of y for the three-chain ladder.

$$\begin{aligned} \epsilon(k_x, \pi)^2 = & \epsilon(0, \pi)^2 \cos^2(k_x/2) + \epsilon(\pi, \pi)^2 \sin^2(k_x/2) \\ & + c_0 \sin^2(k_x). \end{aligned} \quad (9)$$

For $y=1$, the Ising expansions give an energy gap of $\epsilon(\pi, \pi)=0.44(7)$. A more precise estimate is obtained by

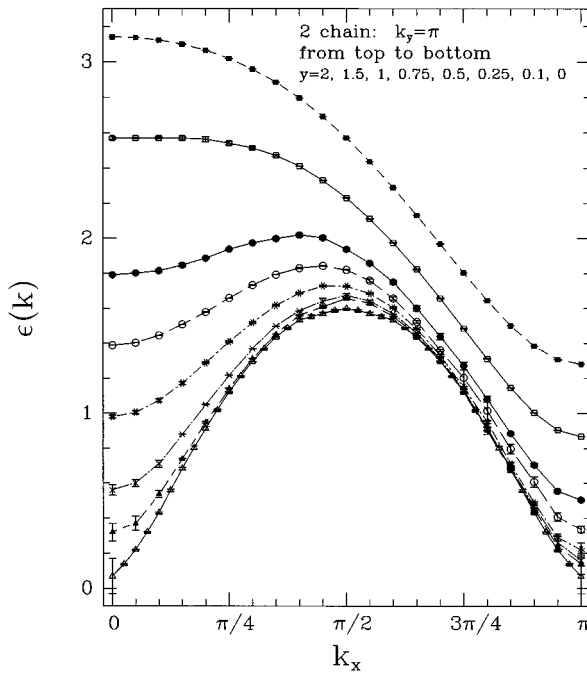


FIG. 4. The dispersions of the spin-triplet excited states of the two-chain ladder with antiferromagnetic interchain coupling $y=2, 1.5, 1, 0.75, 0.5, 0.25, 0.1$, and 0 (shown in the figure from the top to the bottom, respectively), for $k_y=\pi$; the results for $y \geq 1$ are from the dimer expansion, and the results for $y < 1$ are from the Ising expansion.

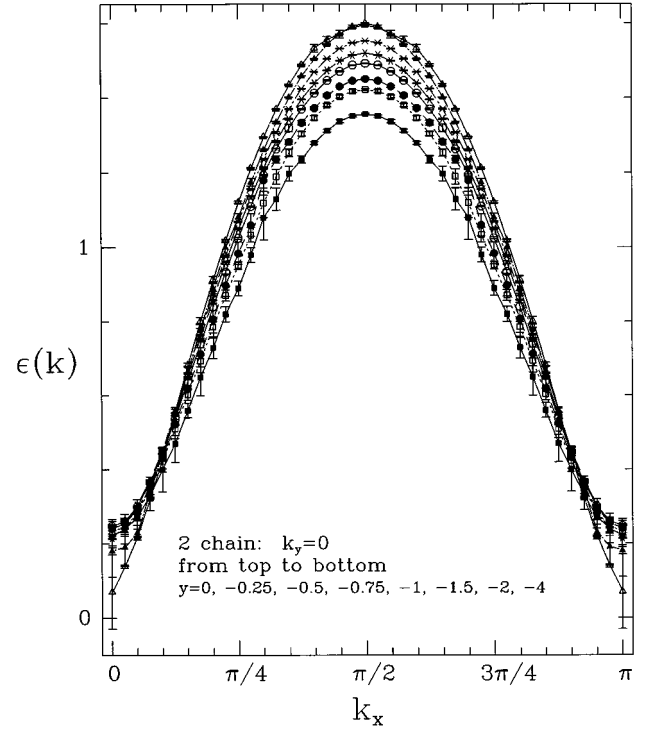


FIG. 5. The $k_y=0$ dispersions of the spin-triplet excited states of the two-chain ladder with ferromagnetic interchain couplings $y=0, -0.25, -0.5, -0.75, -1, -1.5, -2$, and -4 . For the data shown, $\epsilon(\pi/2)$ decreases monotonically with increasing y .

the dimer expansions, which give $\epsilon(\pi, \pi)=0.504(7)$. We will discuss the dimer expansions later.

For ferromagnetic interchain coupling, the two bands of spectra are independent, but each band is a simple cosine function with a gap at the minimum and symmetric about $k_x=\pi/2$, as shown in Figs. 5 and 6. As noted in Fig. 4, it is clear that the spin gap decreases smoothly as y is reduced, and vanishes at $y=0$. These results agree well with previous calculations.⁶

For the three-chain system, there are three bands. In the Ising limit, two bands have initial excitations located in the side rows, and the third band has it in the middle row. Figures 7 and 12 show the spectrum of the three bands for ferromagnetic and antiferromagnetic interchain couplings. From these graphs, we can see that all of the dispersion relations have a simple cosine function (except for the middle row band with large y) with a minimum located at $k_x=0$ (or $k_x=\pi$ by symmetry); where two of these three bands have a definite gap, the third band (the symmetric excitations for the outer chains) is consistent with a gapless spectrum. The estimate for the gap in the third band for all y values is $0.2(3)$ [except for the case of $y=0$ where we got $0.08(10)$]. We note here that we have rather large uncertainties in the gap due to the fact that one class of approximants give values very close to zero, whereas another class of approximants give a much larger value. Hence we cannot exclude the possibility of a finite gap simply from these calculations. But given our earlier results on the phase boundary with Ising anisotropy, we believe the spectra are gapless.

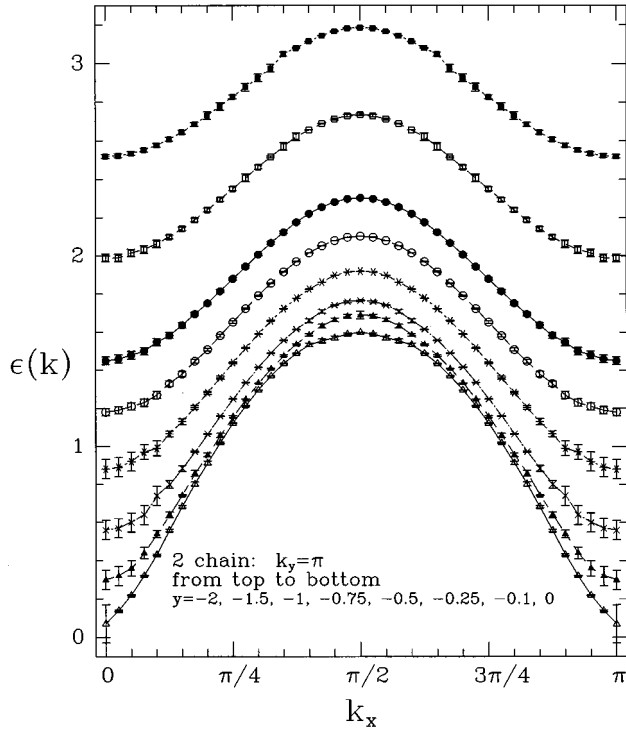


FIG. 6. The dispersions of the spin-triplet excited states of the two-chain ladder with ferromagnetic interchain coupling $y = -2, -1.5, -1, -0.75, -0.5, -0.25, -0.1$, and 0 , for $k_y = \pi$.

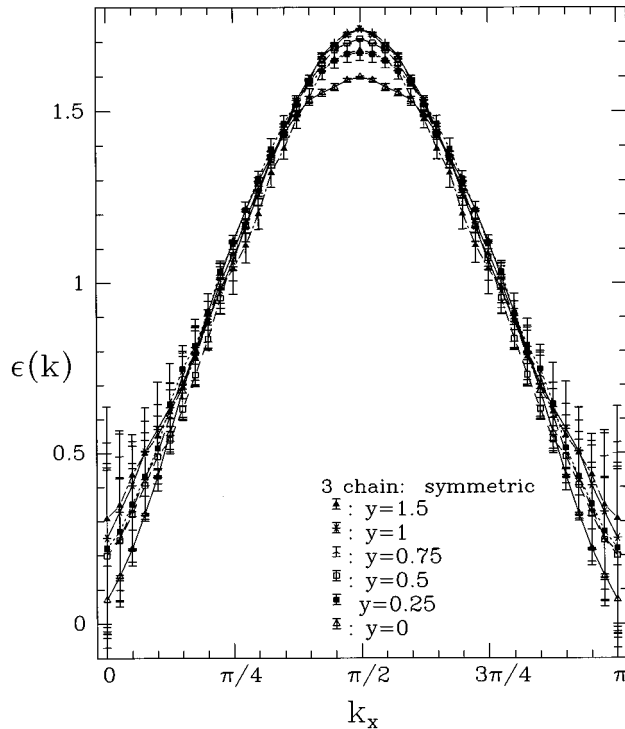


FIG. 7. The dispersions of the spin-triplet excited states of the three-chain ladder with antiferromagnetic interchain coupling $y = 1.5, 1, 0.75, 0.5, 0.25$, and 0 , for symmetric excitations in the outer chains.

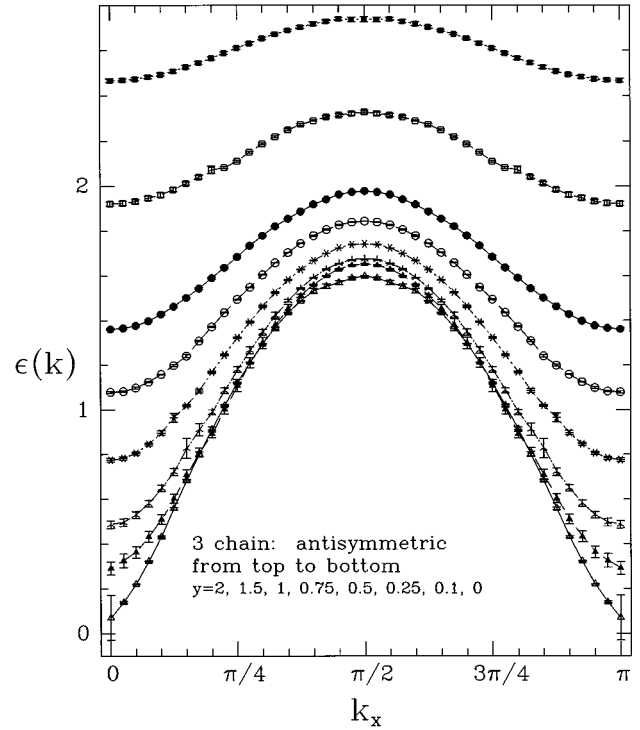


FIG. 8. The dispersions of the spin-triplet excited states of the three-chain ladder with antiferromagnetic interchain coupling $y = 2, 1.5, 1, 0.75, 0.5, 0.25, 0.1$, and 0 , for antisymmetric excitations in the outer chains.

B. Dimer expansions

For two-chain ladders, with antiferromagnetic coupling between the chains, there is an alternative $T=0$ expansion that can be developed. In the limit that the exchange coupling along the rungs J_{\perp} is much larger than the coupling J_{\parallel} along the chains, that is, $y \gg 1$, the rungs interact only weakly with each other, and the dominant configuration in the ground state is the product state with the spin on each rung forming a spin singlet, so the Hamiltonian in Eq. (1) can be rewritten as

$$H/J_{\perp} = H_0 + (1/y)V \quad (10)$$

where

$$H_0 = \sum_{i,l=1}^{l=n_l-1} \mathbf{S}_{l,i} \cdot \mathbf{S}_{l+1,i}, \quad V = \sum_{i,l=1}^{l=n_l} \mathbf{S}_{l,i} \cdot \mathbf{S}_{l,i+1}. \quad (11)$$

We can treat the operator H_0 as the unperturbed Hamiltonian. The eigenstates of a single pair of spins, or dimers, consist of one singlet state with total $S=0$ and eigenenergy $E_s = -3/4$:

$$|\Psi\rangle_s = \frac{1}{\sqrt{2}}(|\uparrow\downarrow\rangle - |\downarrow\uparrow\rangle) \quad (12)$$

and three triplet states with total $S=1$ and eigenenergy $E_t = 1/4$:

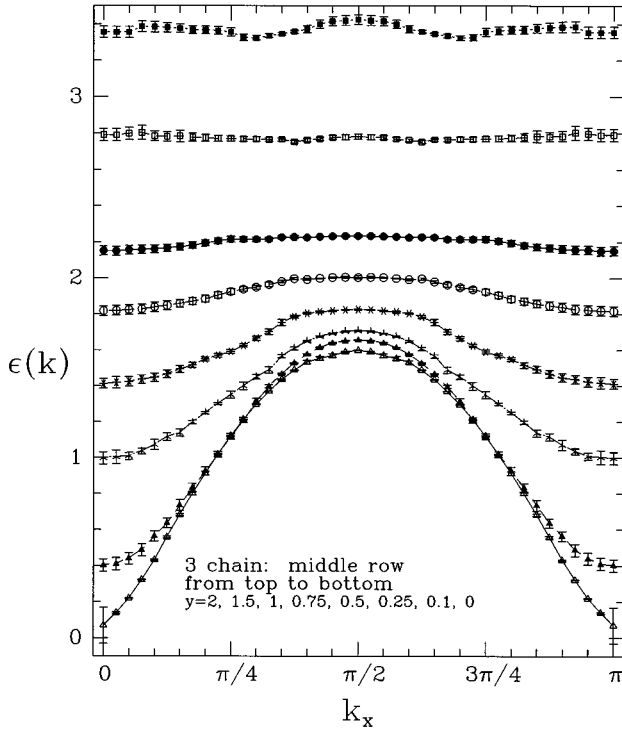


FIG. 9. The dispersions of the spin-triplet excited states of the three-chain ladder with antiferromagnetic interchain coupling $y=2, 1.5, 1, 0.75, 0.5, 0.25, 0.1$, and 0 , for excitations in the middle chain.

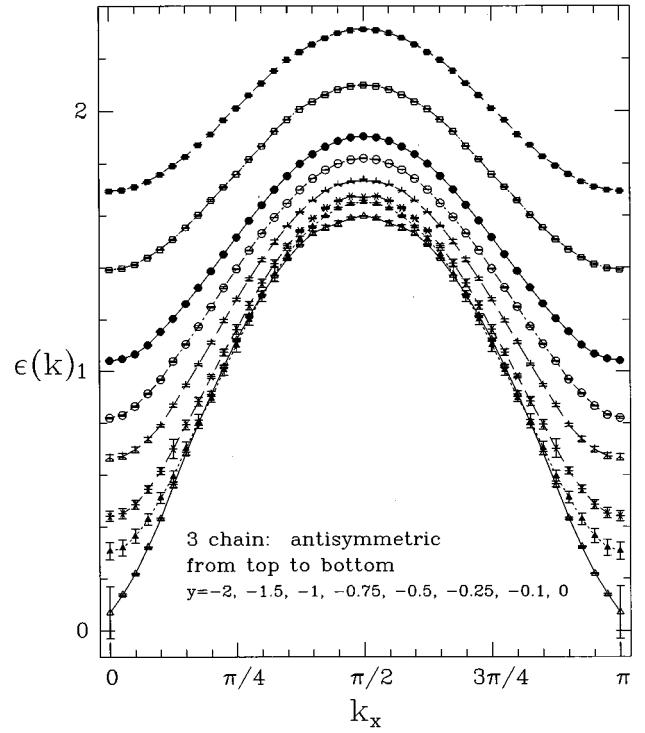


FIG. 11. The dispersions of the spin-triplet excited states of the three-chain ladder with ferromagnetic interchain coupling $y=-2, -1.5, -1, -0.75, -0.5, -0.25, -0.1$, and 0 , for antisymmetric excitations in the outer chains.

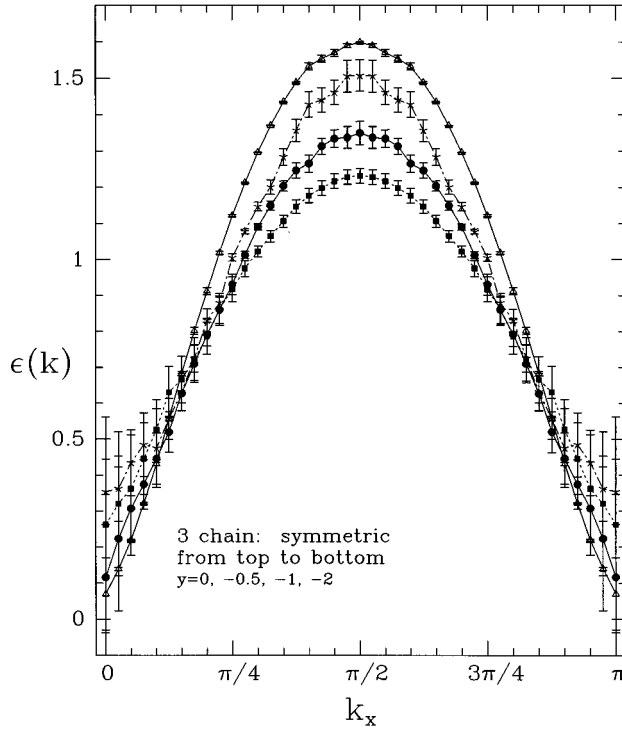


FIG. 10. The dispersions of the spin-triplet excited states of the three-chain ladder with ferromagnetic interchain coupling $y=0, -0.5, -1$, and -2 for symmetric excitations in the outer chains. For the data shown $\epsilon(\pi/2)$ decreases monotonically with increasing y .

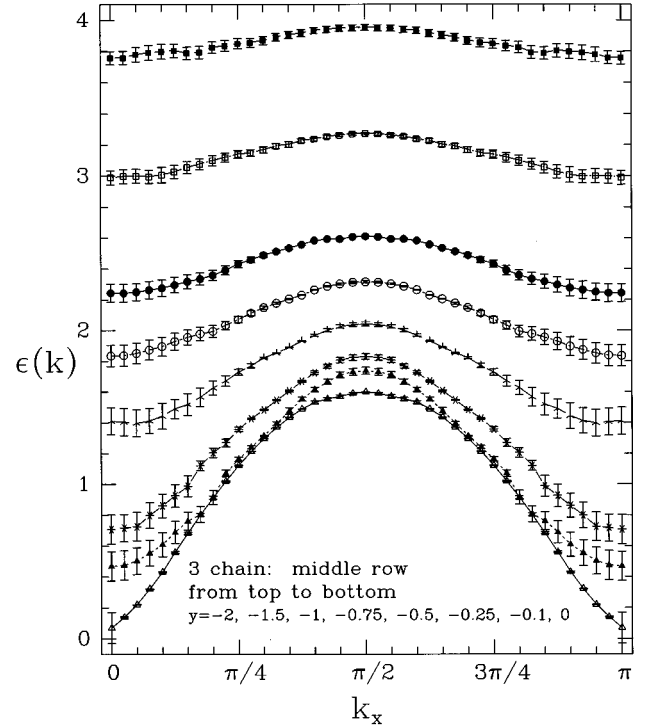


FIG. 12. The dispersions of the spin-triplet excited states of the three-chain ladder with ferromagnetic interchain coupling $y=-2, -1.5, -1, -0.75, -0.5, -0.25, -0.1$, and 0 , for excitations in the middle chain.

TABLE III. Series coefficients for the dimer expansion of the two-chain triplet spin-wave excitation spectrum $\epsilon(k_x, k_y = \pi) = y \sum_{n,m} a_{n,m} (1/y)^n \cos(mk_x)$. Nonzero coefficients $a_{n,m}$ up to order $n=8$ are listed.

(n,m)	$a_{n,m}$	(n,m)	$a_{n,m}$	(n,m)	$a_{n,m}$	(n,m)	$a_{n,m}$
(0, 0)	1.000000000	(5, 1)	$-2.031250000 \times 10^{-1}$	(3, 3)	$1.250000000 \times 10^{-1}$	(5, 5)	$5.468750000 \times 10^{-2}$
(2, 0)	$7.500000000 \times 10^{-1}$	(6, 1)	$9.375000000 \times 10^{-2}$	(4, 3)	$1.250000000 \times 10^{-1}$	(6, 5)	$7.812500000 \times 10^{-2}$
(3, 0)	$3.750000000 \times 10^{-1}$	(7, 1)	$3.293457031 \times 10^{-1}$	(5, 3)	$-9.375000000 \times 10^{-2}$	(7, 5)	$-6.042480469 \times 10^{-2}$
(4, 0)	$-2.031250000 \times 10^{-1}$	(8, 1)	$2.555847168 \times 10^{-1}$	(6, 3)	$-3.164062500 \times 10^{-1}$	(8, 5)	$-2.657165527 \times 10^{-1}$
(5, 0)	$-6.250000000 \times 10^{-1}$	(2, 2)	$-2.500000000 \times 10^{-1}$	(7, 3)	$-2.222900391 \times 10^{-1}$	(6, 6)	$-4.101562500 \times 10^{-2}$
(6, 0)	$-5.000000000 \times 10^{-1}$	(3, 2)	$-2.500000000 \times 10^{-1}$	(8, 3)	$2.752685547 \times 10^{-1}$	(7, 6)	$-6.835937500 \times 10^{-2}$
(7, 0)	$2.966308594 \times 10^{-1}$	(4, 2)	$-3.125000000 \times 10^{-2}$	(4, 4)	$-7.812500000 \times 10^{-2}$	(8, 6)	$4.957580566 \times 10^{-2}$
(8, 0)	1.120300293	(5, 2)	$2.031250000 \times 10^{-1}$	(5, 4)	$-9.375000000 \times 10^{-2}$	(7, 7)	$3.222656250 \times 10^{-2}$
(1, 1)	1.000000000	(6, 2)	$1.718750000 \times 10^{-1}$	(6, 4)	$7.128906250 \times 10^{-2}$	(8, 7)	$6.152343750 \times 10^{-2}$
(3, 1)	$-2.500000000 \times 10^{-1}$	(7, 2)	$-1.728515625 \times 10^{-1}$	(7, 4)	$2.690429688 \times 10^{-1}$	(8, 8)	$-2.618408203 \times 10^{-2}$
(4, 1)	$-3.125000000 \times 10^{-1}$	(8, 2)	$-5.047454834 \times 10^{-1}$	(8, 4)	$1.690521240 \times 10^{-1}$		

$$|\Psi\rangle_t = \left[\frac{1}{\sqrt{2}} (|\uparrow\downarrow\rangle + |\downarrow\uparrow\rangle), |\uparrow\uparrow\rangle, |\downarrow\downarrow\rangle \right]. \quad (13)$$

The operator V is treated as a perturbation. It can cause excitations on a pair of neighboring dimers. Details of the dimer expansions and the matrix elements of V are given in Ref. 19, and will not be repeated here.

We have carried out the dimer expansion for the ground state energy to order $(1/y)^9$ and for the lowest lying triplet excitations to order $(1/y)^8$. The series for the ground state energy per site E_0/N is

$$\begin{aligned} E_0/N = J_{\perp} [& -3/8 - 3/(16y^2) - 3/(32y^3) + 3/(256y^4) \\ & + 45/(512y^5) + 159/(2048y^6) - 879/(32\,768y^7) \\ & - 4527/(32\,768y^8) - 248\,391/(2\,097\,152y^9)] \end{aligned} \quad (14)$$

and the series for the excitation spectrum are listed in Table III. Again, we use the integrated first-order inhomogeneous

TABLE IV. Series coefficients for high temperature series expansion of the uniform susceptibility $\chi(T) = \beta \sum_i c_i \beta^i / (n_i 2^{i+4} i!)$, and the specific heat $C(T) = \beta^2 \sum_i c_i \beta^i / (n_i 2^{i+5} i!)$. Coefficients c_i are listed for two-chain and three-chain ladders with $y=1$.

i	$\chi(T)$ for two-chain	$\chi(T)$ for three-chain	$C(T)$ for two-chain	$C(T)$ for three-chain
0	8	12	36	60
1	-12	-20	72	120
2	12	28	-270	-522
3	6	-20	-2640	-5040
4	-20	4	90	3270
5	-162	-160	141876	318780
6	-630	-1052	580797	1075767
7	9991	17298	-10663200	-28792032
8	88228	80468	-118074186	-291518730
9	-779322	-1467200	946669020	3061122900
10	-13957358	-12792822	26078160405	76820424879
11	55717397	165603440	-42521155560	-195632449272
12	2827957594	2955180058	-6789937647207	-22502126499801
13	4867299659	-24526691326		
14	-687967034169	-924449102836		

differential approximants²² to extrapolate the series. For the ground state energy, we get $E_0/N = -0.5785(5)$ for $y=1$, which agrees very well with the recent quantum Monte Carlo (QMC) result, $E_0/N = -0.5780(2)$, of Frischmuth *et al.*¹⁶ For the excitation spectrum, the dimer expansions give much better results than the Ising expansions for the case of $y > 1$. For $y \sim 1$ the dimer expansions also appear to converge better. The overall spectra determined from the combined study of dimer and Ising expansions are shown in Fig. 4.

C. High temperature series expansions

We now turn to the thermodynamic properties of the ladder system at finite temperatures. We have developed high temperature series expansions for the uniform magnetic susceptibility $\chi(T)$ and the specific heat $C(T)$, for two-chain and three-chain system with $J_{\perp} = J_{\parallel}$,

$$\chi(T) = \frac{\beta}{N} \sum_i \sum_j \frac{\text{Tr} S_i^z S_j^z e^{-\beta H}}{\text{Tr} e^{-\beta H}}, \quad C(T) = \frac{\partial U}{\partial T}, \quad (15)$$

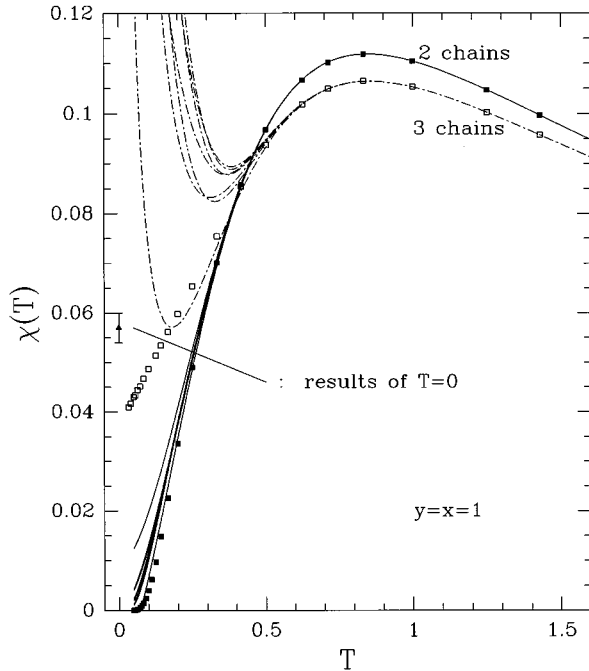


FIG. 13. Susceptibility as a function of temperature for two-chain and three-chain ladders from the high temperature series expansion, and the Ising expansion at $T=0$ (for three-chain ladder only). Several different integrated differential approximants to the high temperature series are shown. Also shown are the QMC results of Frischmuth *et al.* (Ref. 16) as the filled symbols (for two-chain ladder) and open symbols (for three-chain ladder) for comparison.

where N is the number of sites and $\beta=1/(k_B T)$, and the internal energy U is defined by

$$U = \frac{\text{Tr} H e^{-\beta H}}{\text{Tr} e^{-\beta H}}. \quad (16)$$

The series were computed to order β^{14} . The number of contributing graphs, with up to 14 bonds, was 4545 for the two-chain ladders and 5580 for the three-chain ladders. The series are listed in Table IV. We use integrated first-order inhomogeneous differential approximants²² to extrapolate the series. The resulting estimates are shown in Figs. 13 and 14. For the susceptibility, as a comparison, the recent quantum Monte Carlo (QMC) results of Frischmuth *et al.*¹⁶ and the results from our $T=0$ Ising expansion for three chains are also shown. It can be seen that our results agree very well with the QMC results except for the three-chain system at very low temperatures. Given the recent findings that for the spin-half chain the $T=0$ value is reached from finite temperatures with infinite slope,²³ one might expect the $T \rightarrow 0$ behavior for these three-chain systems to be equally complex, making it very difficult to explore numerically. For the specific heat, our results showed good convergence up to the peak, but poor convergence below it. The results for the two-chain ladder are consistent with recent quantum transfer-matrix calculations by Troyer *et al.*¹⁴

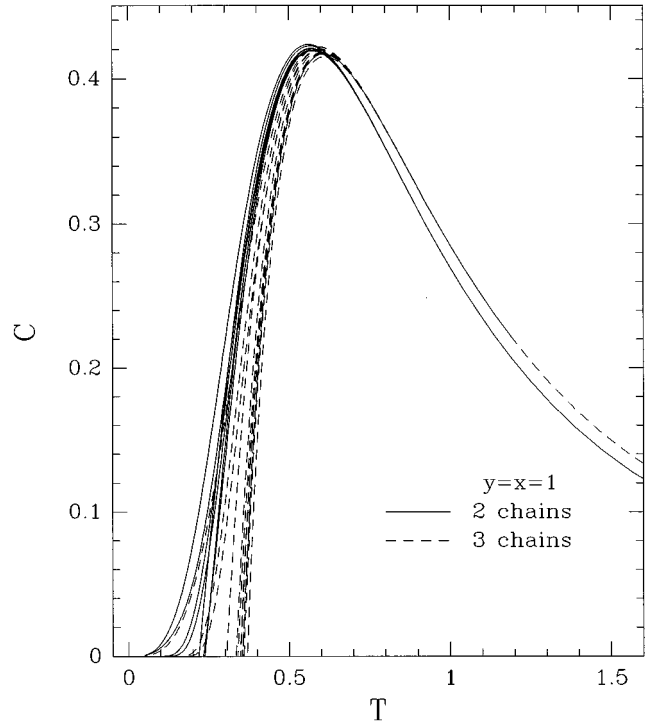


FIG. 14. The specific heat as a function of temperature for two-chain and three-chain ladders from the high temperature series expansion. Several different integrated differential approximants are shown.

III. CONCLUSIONS

We have studied the two- and three-chain Heisenberg-Ising ladders by a variety of different series expansions. Our results confirm the existence of a gap in the excitation spectrum of two-chain systems, with either ferromagnetic or antiferromagnetic interchain interactions. For three-chain systems, a direct calculation of the excitation spectra leads to rather large uncertainties near the minimum and on that basis the possibility of a gap cannot be ruled out. However, given our other results on the phase diagram with Ising anisotropy and the uniform susceptibility, we are led to the conclusion that the spectra are gapless. The $T=0$ phase diagram as well as the temperature dependence of the uniform susceptibility and the specific heat are also calculated. Overall, our results are in reasonable agreement with previous numerical studies of these systems.

ACKNOWLEDGMENTS

This work forms part of a research project supported by a grant from the Australian Research Council. R.R.P.S. is supported in part by the National Science Foundation through Grant No. DMR-9318537 and would like to thank the University of New South Wales for hospitality and the Gordon Godfrey Foundation for support, while the work was being done. We would also like to thank Dr. Troyer for providing us with the Monte Carlo data for comparison.

- *Electronic address: otja@newt.phys.unsw.edu.au
†Electronic address: singh@solid.ucdavis.edu
‡Electronic address: w.zheng@unsw.edu.au
- ¹I. Affleck, M.P. Gelfand, and R.R.P. Singh, *J. Phys. A* **27**, 7313 (1994).
²R.S. Eccleston, T. Barnes, J. Brody, and J.W. Johnson, *Phys. Rev. Lett.* **73**, 2626 (1994).
³M. Takano, Z. Hiroi, M. Azuma, and Y. Takeda, *Jpn. J. Appl. Phys. Ser. 7*, 3 (1992); Z. Hiroi *et al.*, *J. Solid State Chem.* **95**, 230 (1991); T.M. Rice, S. Gopalan, and M. Sigrist, *Europhys. Lett.* **23**, 445 (1993).
⁴E. Dagotto and T.M. Rice (unpublished).
⁵T. Barnes, E. Dagotto, J. Riera, and E. Swanson, *Phys. Rev. B* **47**, 3196 (1993).
⁶T. Barnes and J. Riera, *Phys. Rev. B* **50**, 6817 (1994).
⁷S.R. White, R.M. Noack, and D.J. Scalapino, *Phys. Rev. Lett.* **73**, 886 (1994).
⁸K. Hida (unpublished).
⁹H. Watanabe, *Phys. Rev. B* **50**, 13 442 (1994).
¹⁰M. Azzouz, Liang Chen, and S. Moukouri, *Phys. Rev. B* **50**, 6233 (1994).
¹¹S. Gopalan, T.M. Rice, and M. Sigrist, *Phys. Rev. B* **49**, 8901 (1994).
¹²I. Affleck, *Phys. Rev. B* **37**, 5186 (1988).
¹³A.G. Rojo (unpublished).
¹⁴M. Troyer, H. Tsunetsugu, and D. Würtz, *Phys. Rev. B* **50**, 13 515 (1994).
¹⁵N. Hatano and Y. Nishiyama (unpublished).
¹⁶B. Frischmuth, B. Ammon, and M. Troyer (unpublished).
¹⁷A.W. Sandvik, E. Dagotto, and D.J. Scalapino (unpublished).
¹⁸H.X. He, C.J. Hamer, and J. Oitmaa, *J. Phys. A* **23**, 1775 (1990).
¹⁹M. P. Gelfand, R.R.P. Singh, and D.A. Huse, *J. Stat. Phys.* **59**, 1093 (1990).
²⁰R.R.P. Singh and M.P. Gelfand, *Phys. Rev. Lett.* **61**, 2133 (1988).
²¹M. P. Gelfand (unpublished); R.R.P. Singh and M.P. Gelfand, *Phys. Rev. B* **52**, 15 695 (1995).
²²A.J. Guttmann, in *Phase Transitions and Critical Phenomena*, edited by C. Domb and M.S. Green (Academic, New York, 1989), Vol. 13.
²³S. Eggert, I. Affleck, and M. Takahashi, *Phys. Rev. Lett.* **73**, 332 (1994).